

High-Throughput Selectivity Assays for Small-Molecule Inhibitors of  $\beta$ -Catenin/T-Cell Factor Protein–Protein Interactions

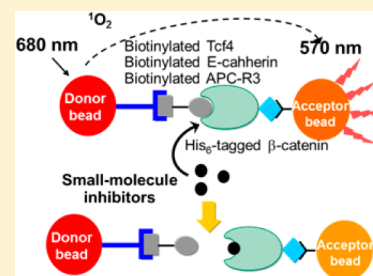
Min Zhang, J. Leon Catrow, and Haitao Ji\*

Department of Chemistry, Center for Cell and Genome Science, University of Utah, Salt Lake City, Utah 84112-0850, United States

## Supporting Information

**ABSTRACT:** Two homogeneous high-throughput assays, AlphaScreen and fluorescence polarization, were established to quantify inhibitor selectivity between different protein–protein complexes. As a first case study, they have been successfully applied to the key protein–protein interactions in the downstream sites of the canonical Wnt signaling pathway. The aberrant formation of the  $\beta$ -catenin/T-cell factor (Tcf) complex is the major driving force for many cancers and fibroses. Crystallographic and biochemical studies reveal that the binding modes of Tcf, E-cadherin, and adenomatous polyposis coli (APC) to  $\beta$ -catenin are identical and mutually exclusive. In the present study, two highly sensitive and robust assays were established to quantitatively evaluate inhibitor selectivity between  $\beta$ -catenin/Tcf,  $\beta$ -catenin/E-cadherin, and  $\beta$ -catenin/APC interactions. A pilot screen demonstrated the feasibility of the assays and yielded four hits for the disruption of  $\beta$ -catenin/Tcf interactions. A potent and dual-selective  $\beta$ -catenin/Tcf inhibitor was identified.

**KEYWORDS:** protein–protein interactions, inhibitor selectivity,  $\beta$ -catenin, E-cadherin, adenomatous polyposis coli, T-cell factor, Wnt signaling, AlphaScreen, fluorescence polarization



Protein–protein interactions (PPIs) play an essential role in most biological processes. Understanding complex PPI networks is one of the foremost challenges of the postgenomic era.<sup>1</sup> The discovery of small-molecule chemical probes that selectively disrupt a single protein–protein interface can greatly facilitate unraveling the structure and dynamic aspects of cellular networks. On the other hand, selective inhibition of PPIs by small molecules provides new drug targets for therapeutic intervention.<sup>2</sup> The proteins tend to use the same interface to interact with the various other proteins, and in pathological conditions, there are high incidences of unexpected PPIs in the densely packed cellular environment. Therefore, there is an urgent need to establish new assays to quantify inhibitor selectivities between different protein–protein complexes. Herein, we reported two robust, high-throughput functional protein assays, AlphaScreen (amplified luminescence proximity homogeneous assay) and fluorescence polarization (FP), to quantify inhibitor selectivity between different protein–protein complexes. These two assays have been applied to the key PPIs in the downstream sites of the canonical Wnt signaling pathway.

The dysregulation of canonical Wnt signaling leads to the initiation and progression of many cancers<sup>3</sup> and fibroses.<sup>4</sup>  $\beta$ -Catenin is the key mediator of the canonical Wnt pathway. In the presence of the Wnt signal, transcriptional coactivator  $\beta$ -catenin enters the cell nucleus and forms a complex with Tcf/Lymphoid enhancer factor (Lef), B-cell lymphoma 9 (BCL9), CREB-binding protein (CBP), and p300. This complex then activates the transcription of Wnt target genes.<sup>5</sup> In the absence of the Wnt signal, cytosolic  $\beta$ -catenin enters a destruction complex formed by Axin, APC, casein kinase I, and glycogen

synthase kinase 3 $\beta$  (GSK3 $\beta$ ) and is actively phosphorylated. Phosphorylated  $\beta$ -catenin is then ubiquitinated, resulting in proteasomal degradation of  $\beta$ -catenin. In addition to its signaling function for the canonical Wnt pathway, cytosolic  $\beta$ -catenin is a structural component of adherens junctions by binding to the cytoplasmic region of E-cadherin.<sup>5</sup> The crystal structures of  $\beta$ -catenin in complexes with Tcf,<sup>6–8</sup> Lef-1,<sup>9</sup> E-cadherin,<sup>10</sup> and APC<sup>11,12</sup> have been determined. These structures reveal that a highly positively charged shallow groove in armadillo repeats 5–9 of  $\beta$ -catenin (residues 142–663 of human  $\beta$ -catenin) forms the essential binding site for Tcf, E-cadherin, and APC. The binding modes of Tcfs, E-cadherin, and APC in this region are identical.<sup>6–12</sup> Biochemical analyses indicated that the binding of Tcf, E-cadherin, and APC to  $\beta$ -catenin is mutually exclusive.<sup>13–15</sup>

Selective inhibition of  $\beta$ -catenin/Tcf PPIs has been recognized as an appealing therapeutic target for anticancer and antifibrotic treatments. Significant efforts have been made to identify small-molecule inhibitors of  $\beta$ -catenin/Tcf interactions; however, very few successful studies have been reported.<sup>16–20</sup> One major challenge in identifying effective  $\beta$ -catenin/Tcf inhibitors is the determination of inhibitor selectivities between  $\beta$ -catenin/Tcf,  $\beta$ -catenin/E-cadherin, and  $\beta$ -catenin/APC PPIs because in normal cells  $\beta$ -catenin/E-cadherin interactions are essential for cell–cell adhesion and  $\beta$ -catenin/APC interactions are critical for  $\beta$ -catenin degradation. In some cancer cells,  $\beta$ -catenin/APC interactions could be of

Received: October 31, 2012

Accepted: January 7, 2013

Published: January 8, 2013

less importance if the key components in the destruction complex for  $\beta$ -catenin degradation are mutated. In breast cancers and many other diseases, however, canonical Wnt signaling is overactivated, and the destruction complex is not mutated; inhibitor selectivity for  $\beta$ -catenin/Tcf over  $\beta$ -catenin/APC interactions is critical.<sup>3</sup> When  $\beta$ -catenin is down-regulated, the armadillo repeats of  $\gamma$ -catenin may form a complex with E-cadherin to rescue adherens junctions.<sup>21</sup> Because the sequence identity between  $\gamma$ -catenin and  $\beta$ -catenin is 79%, inhibitor selectivity over  $\beta$ -catenin/E-cadherin interactions could be projected to that over  $\gamma$ -catenin/E-cadherin interactions. To date, only two cell lysate-based assays, pulldown<sup>17</sup> and coimmunoprecipitation,<sup>16</sup> have been established to qualitatively evaluate the selectivity of  $\beta$ -catenin/Tcf inhibitors. Both assays require multiple steps, and neither can quantify inhibitor potency and selectivity. To facilitate the identification of selective  $\beta$ -catenin/Tcf inhibitors, there is an urgent need for developing new high-throughput screening (HTS) assays that can quantify inhibitor selectivity between  $\beta$ -catenin/Tcf,  $\beta$ -catenin/E-cadherin, and  $\beta$ -catenin/APC PPIs.

An AlphaScreen selectivity assay was established. The schematic description of this assay is shown in Supplementary Figure 1 in the Supporting Information. The streptavidin-coated donor beads and the nickel chelate acceptor beads are brought together through the interactions between biotinylated Tcf, E-cadherin, or APC and His<sub>6</sub>-tagged  $\beta$ -catenin. The  $\beta$ -catenin/Tcf AlphaScreen assay uses human  $\beta$ -catenin (residues 138–686) and human Tcf4 (residues 7–51).<sup>22</sup> The isothermal titration calorimetry (ITC) studies show that the  $K_d$  value of  $\beta$ -catenin and cytoplasmic E-cadherin interactions is 41–82 nM.<sup>15,21</sup> A comparison of the crystal structures of  $\beta$ -catenin in complexes with human Tcf4 (PDB ID, 2GL7),<sup>8</sup> murine E-cadherin (PDB ID, 1I7W),<sup>10</sup> and human APC-R3 (the third 20-amino acid repeat of APC, PDB ID, 1TH1)<sup>12</sup> reveals that the overlapping sequences of Tcf4, E-cadherin, and APC-R3 that bind to the same region of  $\beta$ -catenin are L12–V49 of human Tcf4, A826–L850 of murine E-cadherin, and L1482–L1511 of human APC-R3, respectively. Segment D862–A875 of murine E-cadherin was observed to form two additional antiparallel helices to pack against the exposed hydrophobic core residues of the first armadillo repeat of  $\beta$ -catenin.<sup>10</sup> Residues 819–873 of human E-cadherin correspond to residues 821–875 of murine E-cadherin. Therefore, C-terminally biotinylated human E-cadherin (residues 819–873) and N-terminally His<sub>6</sub>-tagged human  $\beta$ -catenin (residues 138–686) were used in the  $\beta$ -catenin/E-cadherin AlphaScreen assay.

Because the expected  $K_d$  value of  $\beta$ -catenin/E-cadherin interactions (41–82 nM) is higher than the binding capacity of the streptavidin-coated beads (15 nM for 10  $\mu$ g/mL beads), a competitive binding assay was used to determine the apparent  $K_d$  value of AlphaScreen. The concentrations of His<sub>6</sub>-tagged  $\beta$ -catenin and biotinylated E-cadherin were set to 0.5 and 5 nM, respectively, and different concentrations of unlabeled E-cadherin peptide were added to determine the  $IC_{50}$  value. As shown in Figure 1A, the apparent  $K_d$  value of  $\beta$ -catenin/E-cadherin is  $60.1 \pm 3.1$  nM, which is in good agreement with the  $K_d$  value of native  $\beta$ -catenin/E-cadherin interactions from the ITC study.<sup>15,21</sup>

The cross-titration study showed that the S/B ratios of 40 nM  $\beta$ -catenin were 116.18 ( $S = 1307123 \pm 11534$ ,  $B = 11251 \pm 224$ , Supplementary Figure 2A in the Supporting Information). With the intention to keep the concentration of biotinylated E-cadherin low for the competitive inhibition assay while

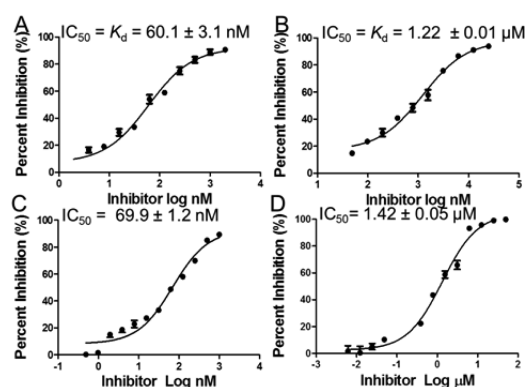


**Figure 1.** (A and B) AlphaScreen competitive binding assays to determine the apparent  $K_d$  values. (A)  $\beta$ -Catenin/E-cadherin interaction; (B)  $\beta$ -catenin/APC interactions. (C and D) AlphaScreen competitive inhibition experiments to determine assay specificity. (C) Unlabeled E-cadherin for  $\beta$ -catenin/E-cadherin interaction; (D) unlabeled APC-R3 for  $\beta$ -catenin/APC-R3 interactions. Each set of data was expressed as the mean  $\pm$  standard deviation ( $n = 3$ ).

maintaining a high assay signal and sensitivity, 10 nM biotinylated E-cadherin and 40 nM His<sub>6</sub>-tagged  $\beta$ -catenin were used in the competitive inhibition assay. To validate the ability of the  $\beta$ -catenin/E-cadherin AlphaScreen assay to evaluate inhibitors, unlabeled human E-cadherin peptide (residues 819–873) was used to displace biotinylated E-cadherin (residues 819–873) from  $\beta$ -catenin. As shown in Figure 1C, unlabeled E-cadherin peptide can effectively disrupt the binding of biotinylated E-cadherin to His<sub>6</sub>-tagged  $\beta$ -catenin in a concentration-dependent manner with an  $IC_{50}$  of  $69.9 \pm 1.2$  nM.

APC encodes a large 310 kDa protein with multiple domains. The third 20-amino acid repeat, APC-R3, is the tightest binder with a  $K_d$  of 3.1  $\mu$ M for full-length  $\beta$ -catenin in the ITC study.<sup>11,15</sup> The crystallographic and biochemical studies of  $\beta$ -catenins/APC-R3 PPIs reveal that human APC-R3 segment Q1477–K1518 closely contacts with  $\beta$ -catenin.<sup>11,12</sup> The C-terminally fluorescein-labeled human APC-R3 (residues 1477–1519) and N-terminally His<sub>6</sub>-tagged human  $\beta$ -catenin (residues 138–686) were used in the AlphaScreen selectivity assay. Because the expected  $K_d$  value of  $\beta$ -catenin/APC-R3 PPIs (3.1  $\mu$ M) is higher than the binding capacity of the beads, a competitive binding assay was conducted to determine the apparent  $K_d$  value. The concentrations of His<sub>6</sub>-tagged  $\beta$ -catenin and biotinylated APC-R3 were set to 3 and 30 nM, respectively, and different concentrations of unlabeled APC-R3 peptide were examined. As shown in Figure 1B, the apparent  $K_d$  value of  $\beta$ -catenin/APC-R3 is  $1.22 \pm 0.01$   $\mu$ M, which is in good agreement with the  $K_d$  value of native  $\beta$ -catenin/APC-R3 interactions from the ITC study.<sup>11,15</sup>

The cross-titration study showed that the S/B ratio of 40 nM  $\beta$ -catenin was 105.99 ( $S = 1575131 \pm 18758$ ,  $B = 14861 \pm 315$ , Supplementary Figure 2B in the Supporting Information). With the intention to keep the concentration of biotinylated APC-R3 low and maintain a high assay signal and sensitivity, 10 nM biotinylated APC-R3 and 40 nM His<sub>6</sub>-tagged  $\beta$ -catenin were used in inhibitor assay. To validate the ability of the  $\beta$ -catenin/APC-R3 AlphaScreen assay in evaluating inhibitors, unlabeled human APC-R3 peptide (residues 1477–1519) was used to displace biotinylated APC-R3 (residues 1477–1519) from  $\beta$ -catenin. As shown in Figure 1D, unlabeled APC-R3 peptide can effectively disrupt the binding of biotinylated APC-R3 to His<sub>6</sub>-

tagged  $\beta$ -catenin in a concentration-dependent manner with an  $IC_{50}$  of  $1.42 \pm 0.05 \mu\text{M}$ .

The stability of assay signal over time is an important parameter in the HTS selectivity assay. We have reported that the  $\beta$ -catenin/Tcf AlphaScreen assay was stable over 24 h in the previous study.<sup>22</sup> In this study, the time dependence of  $\beta$ -catenin/E-cadherin and  $\beta$ -catenin/APC-R3 AlphaScreen signals was evaluated over a 24 h period following the addition of the donor beads. All signals were stable under the examined conditions over the course of 24 h with the maximum and midpoint signals peaking at 5 h and only showing a slight reduction after 5 h (Supplementary Figure 3 in the Supporting Information). These results demonstrate that plate reading can be performed overnight, and the new AlphaScreen selectivity assays are compatible with off-line microplate reading.

Statistic parameter  $Z'$  was calculated to reflect the dynamic range and signal deviations of the newly established HTS selectivity assays. The closer the  $Z'$  factor to 1, the higher the assay quality with a typical cutoff  $Z'$  value of 0.5 for the acceptable HTS assays. As reported previously, the  $\beta$ -catenin/Tcf AlphaScreen assay exhibits a  $Z'$  factor of 0.87.<sup>22</sup> Figure 2A

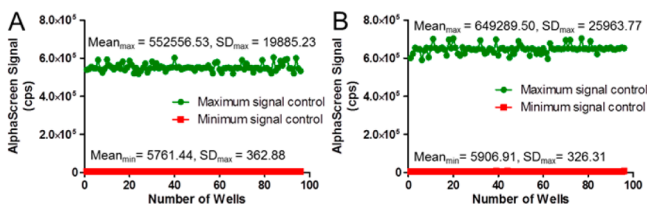


**Figure 2.** Determination of the  $Z'$  factors of the new AlphaScreen assays. (A)  $\beta$ -Catenin/E-cadherin interactions; (B)  $\beta$ -catenin/APC-R3 interactions.

shows that the  $\beta$ -catenin/E-cadherin AlphaScreen assay has a  $Z'$  factor of 0.89. The  $\beta$ -catenin/APC-R3 AlphaScreen assay has a  $Z'$  factor of 0.88 (Figure 2B). Because DMSO is a common solvent to prepare stock solutions for inhibitor candidates, DMSO tolerance for the HTS selectivity assays was examined. No significant differences were observed for the  $K_d$  values and the S/B ratios of  $\beta$ -catenin/E-cadherin and  $\beta$ -catenin/APC-R3 PPIs up to 4% DMSO (Supplementary Figure 4 in the Supporting Information). No significant differences were observed for the  $IC_{50}$  values of unlabeled E-cadherin to the  $\beta$ -catenin/E-cadherin assay and unlabeled APC-R3 to the  $\beta$ -catenin/APC-R3 assay up to 4% DMSO. These data were consistent with what were observed in the  $\beta$ -catenin/Tcf assay.<sup>22</sup> All of these data indicate the suitability of these AlphaScreen assays for the HTS selectivity assay.

A complementary FP HTS selectivity assay was established to reduce the disturbance from metal chelators, biotin mimetics, or singlet oxygen quenchers to AlphaScreen. A schematic description of the FP selectivity assay is shown in Supplementary Figure 5 in the Supporting Information. The  $\beta$ -catenin/Tcf FP assay uses human  $\beta$ -catenin (residues 138–686) and human Tcf4 (residues 7–51).<sup>22</sup> In the FP assay of  $\beta$ -catenin/E-cadherin interactions, C-terminally fluorescein-labeled human E-cadherin (residues 819–873) and human  $\beta$ -catenin (residues 138–686) were used. Three concentrations, 2.5, 5, and 10 nM E-cadherin fluorescent tracer, were examined in the saturation binding experiment. These concentrations are significantly lower than the  $K_d$  value ( $K_d = 41$ – $82$  nM) from the ITC study<sup>15,21</sup> but adequate to give significant relative fluorescence intensity to provide a good S/B ratio. As shown in

Figure 3A, the apparent  $K_d$  values of 2.5, 5, and 10 nM E-cadherin fluorescent tracers and  $\beta$ -catenin were  $82.3 \pm 2.2$ ,  $80.4$

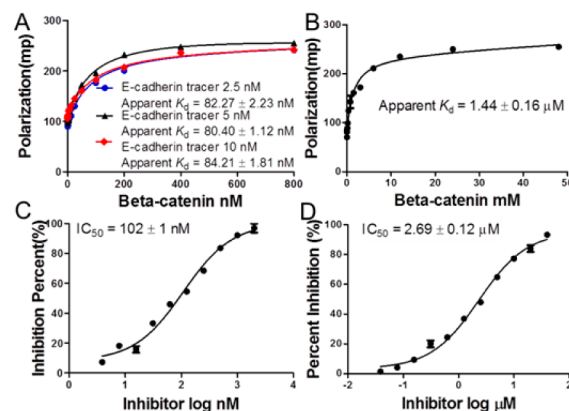


**Figure 3.** (A and B) Saturation experiment to determine the apparent  $K_d$  values of new FP assays. (A) E-cadherin/ $\beta$ -catenin interactions; (B) APC-R3/ $\beta$ -catenin interactions. (C and D) FP competitive inhibition experiments to determine assay specificity. (C) Unlabeled E-cadherin peptide for E-cadherin/ $\beta$ -catenin interactions; (D) unlabeled APC-R3 peptide for  $\beta$ -catenin/APC-R3 interactions. Each set of data was expressed as the mean  $\pm$  standard deviation ( $n = 3$ ).

$\pm 1.1$ , and  $84.2 \pm 1.8$  nM, respectively, which are in good agreement with the ITC  $K_d$  value.<sup>15,21</sup>

The FP signal window of 5 nM E-cadherin tracer (152 mP) is larger than those of 2.5 and 10 nM E-cadherin tracers (141 and 113 mP, respectively), offering a better assay range. With the intention of keeping the concentration of E-cadherin fluorescent tracer as low as possible while maintaining high fluorescence signal and assay sensitivity, 5 nM E-cadherin fluorescent tracer and 150 nM  $\beta$ -catenin were chosen for the FP competitive inhibition assay. Moreover, this concentration of the E-cadherin tracer offers strong fluorescence intensity that can overcome the potential interference of the weekly fluorescent compounds. To validate the  $\beta$ -catenin/E-cadherin competitive inhibition assays, the ability of unlabeled human E-cadherin peptide (residues 819–873) to displace E-cadherin fluorescent tracer (residues 819–873) from  $\beta$ -catenin was examined. As shown in Figure 3C, unlabeled E-cadherin peptide can effectively compete the binding of E-cadherin fluorescent tracer to  $\beta$ -catenin in a concentration-dependent manner with an  $IC_{50} = 102 \pm 1$  nM.

C-terminally fluorescein-labeled human APC-R3 (residues 1477–1519) and human  $\beta$ -catenin (residues 138–686) were used for the  $\beta$ -catenin/APC-R3 FP assay. The saturation binding assay derived an apparent  $K_d$  value of  $1.44 \pm 0.16 \mu\text{M}$  (Figure 3B), which is in good agreement with the ITC  $K_d$  value of native  $\beta$ -catenin/APC-R3 interactions.<sup>11,15</sup> On the basis of the derived apparent  $K_d$  value and the effective window of the polarization signals determined by the bound and free fluorescent tracers,  $1.44 \mu\text{M}$   $\beta$ -catenin and 5 nM APC-R3 fluorescent tracer were used in the FP inhibitor assay. To validate the  $\beta$ -catenin/APC-R3 FP competitive inhibition assays, the ability of unlabeled human APC-R3 peptide (residues 1477–1519) to displace APC-R3 fluorescent tracer (residues 1477–1519) from  $\beta$ -catenin was examined. As shown in Figure 3D, unlabeled APC-R3 peptide can competitively inhibit the binding of APC-R3 fluorescent tracer from  $\beta$ -catenin in a concentration-dependent manner with an  $IC_{50} = 2.69 \pm 0.12 \mu\text{M}$ .

The stability of the FP signals over time was assessed by incubating the plate at room temperature over a 24 h period. Previously, we demonstrated the stability of the  $\beta$ -catenin/Tcf FP assay over 24 h.<sup>22</sup> In this study, the stabilities of the  $\beta$ -catenin/E-cadherin and  $\beta$ -catenin/APC-R3 FP assays over 24 h were evaluated. No significant changes in the  $K_d$  values or the dynamic ranges between the highest and the lowest polarization signals ( $\Delta mP$ ) were observed, indicating that this FP selectivity assay is compatible with off-line microplate reading (Supplementary Figure 6 in the Supporting Information).

Statistical parameter  $Z'$  was calculated to assess the precision and robustness of these FP assays for use as the HTS selectivity assays. As shown in Figure 4, the  $Z'$  values of the  $\beta$ -catenin/E-

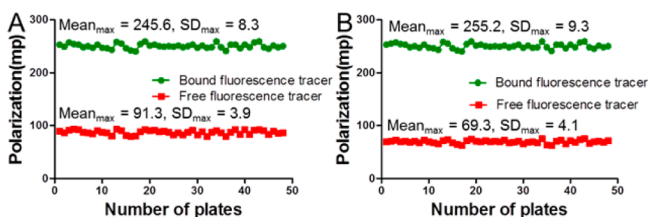


**Figure 4.** Determination of the  $Z'$  factors of the new FP assays. (A)  $\beta$ -Catenin/E-cadherin interactions; (B)  $\beta$ -catenin/APC-R3 interactions. The  $Z'$  factors for each plate are shown in Supplementary Figure 8 in the Supporting Information.

cadherin and  $\beta$ -catenin/APC-R3 FP assays were 0.76 and 0.78, respectively. In the previous study, the  $Z'$  value of the  $\beta$ -catenin/Tcf FP assay was reported as 0.79.<sup>22</sup> DMSO tolerances for the  $\beta$ -catenin/Tcf,  $\beta$ -catenin/E-cadherin, and  $\beta$ -catenin/APC-R3 FP assays were also examined. No significant differences of DMSO on the  $K_d$  values, the S/B ratios, and the  $IC_{50}$  values were observed up to 4% DMSO (Supplementary Figure 7 in the Supporting Information). These data indicate the suitability of these FP assays for the HTS selectivity assay.

To date, four HTS studies have been reported on identifying small-molecule inhibitors for  $\beta$ -catenin/Tcf PPIs.<sup>16–19</sup> An ELISA-based HTS of natural product libraries identified six  $\beta$ -catenin/Tcf inhibitors.<sup>16</sup> Among these six inhibitors, PKF115-584 and CGP049090 can effectively block the expression of Wnt target genes. PKF118-310, with a molecular weight of 193.06, is a very potent  $\beta$ -catenin/Tcf inhibitor, although its inhibition on the expression of Wnt target genes is less effective. Recently, we reported the rational design and synthesis of a small molecule, **1**, based on the bioisosteric replacement of D16 and E17 of human Tcf4.<sup>20</sup> The AlphaScreen assays were performed to quantify the selectivities of these four small-molecule inhibitors for  $\beta$ -catenin/Tcf over  $\beta$ -catenin/E-cadherin and  $\beta$ -catenin/APC interactions. A counterscreen was conducted to identify compounds that interfered with the assay by acting as metal chelators, biotin mimetics, or singlet oxygen quenchers. It was shown that PKF115-584 interfered with the AlphaScreen assay (Supplementary Figure 9 in the Supporting Information). The concentration-dependent inhibitions were observed for all of the other three inhibitors. The results are summarized in Table 1A.

The FP assays were also performed to quantify the selectivities of these four small-molecule inhibitors. The fluorescence backgrounds of these four compounds were very low (<5%) at the detection wavelength. The concentration-

**Table 1.** Inhibitor Selectivities of Small-Molecule  $\beta$ -Catenin/Tcf4 Inhibitors Determined by (A) the AlphaScreen Assay and (B) the FP Assay

compds	$K_i \pm SD$ ( $\mu M$ )			selectivity	
	$\beta$ -catenin/Tcf4	$\beta$ -catenin/E-cadherin	$\beta$ -catenin/APC-R3	Tcf/cadherin	Tcf/APC
A					
CGP049090	$5.9 \pm 1.0$	$12 \pm 1$	$8.3 \pm 1.1$	2.0	1.4
PKF118-310	$3.7 \pm 0.7$	$20 \pm 2$	$66 \pm 3$	5.4	17.8
<b>1</b>	$3.8 \pm 0.5$	$110 \pm 10$	$170 \pm 10$	28.9	44.7
B					
PKF115-584	$18 \pm 2$	$13 \pm 1$	$54 \pm 1$	0.7	3.0
CGP049090	$36 \pm 1$	$14 \pm 1$	$63 \pm 1$	0.4	1.8
PKF118-310	$5.8 \pm 0.2$	$13 \pm 1$	$170 \pm 10$	2.2	29.3
<b>1</b>	$3.1 \pm 0.5$	$100 \pm 10$	$180 \pm 10$	32.3	58.1

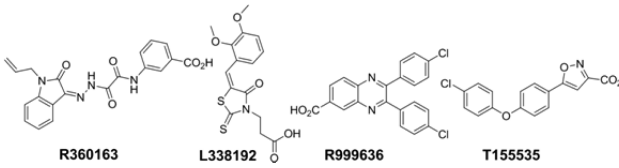
dependent inhibitions were observed for all of the four inhibitors in the FP assay. The results are summarized in Table 1B.

Both the AlphaScreen and the FP assay results indicate that PKF115-584 and CGP049090 have no selectivity for  $\beta$ -catenin/Tcf over  $\beta$ -catenin/APC interactions, while PKF118-310 exhibits 17.8- and 29.3-fold selectivities in the AlphaScreen and FP assays, respectively (Table 1). These results are in good agreement with those of the previous coimmunoprecipitation study.<sup>16</sup> None of PKF115-584, CGP049090, and PKF118-310 exhibits significant selectivity for  $\beta$ -catenin/Tcf over  $\beta$ -catenin/E-cadherin interactions in our AlphaScreen and FP assays, which is surprisingly in contrast to the previous coimmunoprecipitation study.<sup>16</sup> One possible explanation for this striking difference is the different sources of the analyzed E-cadherin proteins. The E-cadherin protein used in the coimmunoprecipitation study was from cell lysates. The protein could be phosphorylated in cell by kinases casein kinase II and GSK-3 $\beta$  before the lysis. The crystal structure of  $\beta$ -catenin in a complex with E-cadherin also indicates that the  $\beta$ -catenin binding region of E-cadherin can be extensively phosphorylated.<sup>10</sup> The  $K_d$  value of the phosphorylated E-cadherin for  $\beta$ -catenin is 3 orders of magnitude lower than the unphosphorylated E-cadherin.<sup>15</sup> A higher phosphorylation state of cellular E-cadherin causes a much tighter binding with  $\beta$ -catenin, which might explain the different selectivity profiles of PKF115-584, CGP049090, and PKF118-310 in the coimmunoprecipitation and AlphaScreen/FP assays. The  $K_i$  values of **1** for disrupting  $\beta$ -catenin/Tcf interactions are  $3.8 \pm 0.5$  and  $3.1 \pm 0.5$   $\mu M$  in the AlphaScreen and FP assays, respectively. The selectivities of **1** for  $\beta$ -catenin/Tcf over  $\beta$ -catenin/E-cadherin and  $\beta$ -catenin/APC-R3 interactions are about 30- and 50-fold, respectively. This compound exhibits the highest dual selectivity among these four inhibitors.

A pilot screen was further performed (Supplementary Figure 10 in the Supporting Information). The crystallographic analyses reveal that an acidic residue-rich segment of Tcf (D<sup>16</sup>-E<sup>24</sup> of human Tcf4) is key for binding to  $\beta$ -catenin.<sup>6–8</sup> A collection of Sigma-Aldrich compounds that contains aromatic and aliphatic carboxylic acids and sulfonamides was assayed. Only the compounds that meet two selection criteria were kept:

(1)  $K_i \leq 80 \mu\text{M}$  for  $\beta$ -catenin/Tcf4 interactions and (2) inhibitor selectivities for  $\beta$ -catenin/Tcf over  $\beta$ -catenin/E-cadherin and  $\beta$ -catenin/APC interactions  $>1$ , respectively. In the AlphaScreen assay, five hits were identified from the primary assay and then subjected to counterscreen. One compound (20%) interferes with the assay, and four hits (hit rate = 1.6%) were identified (Table 2A). In the FP assay, seven

**Table 2. Pilot Screen To Identify New Selective  $\beta$ -Catenin/Tcf Inhibitors with (A) the AlphaScreen Assay and (B) the FP Assay**



comps	$K_i \pm \text{SD} (\mu\text{M})$			selectivity	
	$\beta$ -catenin/Tcf4	$\beta$ -catenin/E-cadherin	$\beta$ -catenin/APC-R3	Tcf/cadherin	Tcf/APC
A					
R360163	21 $\pm$ 1	68 $\pm$ 2	220 $\pm$ 10	3.3	10.5
L338192	29 $\pm$ 1	140 $\pm$ 10	110 $\pm$ 10	4.8	3.8
R999636	13 $\pm$ 1	28 $\pm$ 2	71 $\pm$ 4	2.2	5.5
T155535	21 $\pm$ 1	59 $\pm$ 2	110 $\pm$ 10	2.8	5.2
B					
R360163	16 $\pm$ 1	260 $\pm$ 10	400 $\pm$ 10	16.3	25.0
R999636	8.8 $\pm$ 0.5	51 $\pm$ 1	69 $\pm$ 2	5.8	7.8
T155535	77 $\pm$ 1	87 $\pm$ 1	180 $\pm$ 10	1.1	2.3

hits were identified in the primary assay. The counterscreen removed two compounds (29%). A further analysis identified three hits (hit rate = 1.2%) have statistically “well-fitted” curves ( $0.7 \leq \text{Hill coefficient} \leq 1.3$  and  $r^2 \geq 0.9$ ) (Table 2B). All identified hits have excellent reproducibility in the triplicate runs. A comparison of the AlphaScreen and FP assay results shows that three common hits were identified. L338192 was missed by the FP assay due to its high fluorescence background.

To our best knowledge, no assay has been established to quantitatively evaluate inhibitor selectivity for  $\beta$ -catenin/Tcf over  $\beta$ -catenin/E-cadherin and  $\beta$ -catenin/APC interactions. In the present study, two robust, homogeneous, and quantitative selectivity assays were established. These two assays are simple to run, low cost, and rapid; they are suitable for adaptation to HTS. This study lays the foundation for the discovery of selective small-molecule inhibitors specific for  $\beta$ -catenin/Tcf interactions. A newly discovered potent  $\beta$ -catenin/Tcf inhibitor, **1**, was identified dual selective for  $\beta$ -catenin/Tcf over  $\beta$ -catenin/E-cadherin and  $\beta$ -catenin/APC interactions. This compound provides an excellent starting point to generate more potent and selective inhibitors specific for  $\beta$ -catenin/Tcf PPIs. A pilot screen demonstrated the feasibility of the newly established selectivity assay and yielded four new hits for the disruption of  $\beta$ -catenin/Tcf interactions.

## ■ ASSOCIATED CONTENT

### Supporting Information

Supplementary Figures 1–10 and the experimental details. This material is available free of charge via the Internet at <http://pubs.acs.org>.

## ■ AUTHOR INFORMATION

### Corresponding Author

\*E-mail: [markji@chem.utah.edu](mailto:markji@chem.utah.edu).

### Funding

This project was in part financed by the Pulmonary Fibrosis Foundation I. M. Rosenzweig Young Investigator Award (Award Number, 235170).

### Notes

The authors declare no competing financial interest.

## ■ ACKNOWLEDGMENTS

We thank Professor Wenqing Xu at the University of Washington for  $\beta$ -catenin cDNA and Dr. Hanqing Liu at St. Andrew University, United Kingdom, for pEHISTEV vector.

## ■ REFERENCES

- (1) Vidal, M.; Cusick, M. E.; Barabási, A.-L. Interactome networks and human disease. *Cell* **2011**, *144*, 986–998.
- (2) Wells, J. A.; McClendon, C. L. Reaching for high-hanging fruit in drug discovery at protein-protein interfaces. *Nature* **2007**, *450*, 1001–1009.
- (3) Clevers, H.; Nusse, R. Wnt/ $\beta$ -catenin signaling and disease. *Cell* **2012**, *149*, 1192–1205.
- (4) Akhmetshina, A.; Palumbo, K.; Dees, C.; Bergmann, C.; Venalis, P.; Zerr, P.; Horn, A.; Kireva, T.; Beyer, C.; Zwerina, J.; Schneider, H.; Sadowski, A.; Riener, M.-O.; MacDougald, O. A.; Distler, O.; Schett, G.; Distler, J. H. Activation of canonical Wnt signalling is required for TGF- $\beta$ -mediated fibrosis. *Nat. Commun.* **2012**, *3*, 735.
- (5) Pokutta, S.; Weis, W. I. Structure and mechanism of cadherins and catenins in cell-cell contacts. *Annu. Rev. Cell Dev. Biol.* **2007**, *23*, 237–261.
- (6) Graham, T. A.; Weaver, C.; Mao, F.; Kimelman, D.; Xu, W. Crystal structure of a  $\beta$ -catenin/Tcf complex. *Cell* **2000**, *103*, 885–896.
- (7) Poy, F.; Lepourcelet, M.; Shivdasani, R. A.; Eck, M. J. Structure of a human Tcf4- $\beta$ -catenin complex. *Nat. Struct. Biol.* **2001**, *8*, 1053–1057.
- (8) Sampietro, J.; Dahlberg, C. L.; Cho, U. S.; Hinds, T. R.; Kimelman, D.; Xu, W. Crystal structure of a  $\beta$ -catenin/BCL9/Tcf4 complex. *Mol. Cell* **2006**, *24*, 293–300.
- (9) Sun, J.; Weis, W. I. Biochemical and structural characterization of  $\beta$ -catenin interactions with nonphosphorylated and CK2-phosphorylated Lef-1. *J. Mol. Biol.* **2011**, *405*, 519–530.
- (10) Huber, A. H.; Weis, W. I. The structure of the  $\beta$ -catenin/E-cadherin complex and the molecular basis of diverse ligand recognition by  $\beta$ -catenin. *Cell* **2001**, *105*, 391–402.
- (11) Ha, N.-C.; Tonzuka, T.; Stamos, J. L.; Choi, H.-J.; Weis, W. I. Mechanism of phosphorylation-dependent binding of APC to  $\beta$ -catenin and its role in  $\beta$ -catenin degradation. *Mol. Cell* **2004**, *15*, 511–521.
- (12) Xing, Y.; Clements, W. K.; Le Trong, I.; Hinds, T. R.; Stenkamp, R.; Kimelman, D.; Xu, W. Crystal structure of a  $\beta$ -catenin/APC complex reveals a critical role for APC phosphorylation in APC function. *Mol. Cell* **2004**, *15*, 523–533.
- (13) Hülsken, J.; Birchmeier, W.; Behrens, J. E-cadherin and APC compete for the interaction with  $\beta$ -catenin and the cytoskeleton. *J. Cell Biol.* **1994**, *127*, 2061–2069.
- (14) Omer, C. A.; Miller, P. J.; Diehl, R. E.; Kral, A. M. Identification of Tcf4 residues involved in high-affinity  $\beta$ -catenin binding. *Biochem. Biophys. Res. Commun.* **1999**, *256*, 584–590.
- (15) Choi, H.-J.; Huber, A. H.; Weis, W. I. Thermodynamics of  $\beta$ -catenin-ligand interactions: the roles of the N- and C-terminal tails in modulating binding affinity. *J. Biol. Chem.* **2006**, *281*, 1027–1038.
- (16) Lepourcelet, M.; Chen, Y.-N. P.; France, D. S.; Wang, H.; Crews, P.; Petersen, F.; Bruseo, C.; Wood, A. W.; Shivdasani, R. A.

Small-molecule antagonists of the oncogenic Tcf/ $\beta$ -catenin protein complex. *Cancer Cell* **2004**, *5*, 91–102.

(17) Gonsalves, F. C.; Klein, K.; Carson, B. B.; Katz, S.; Ekas, L. A.; Evans, S.; Nagourney, R.; Cardozo, T.; Brown, A. M.; DasGupta, R. An RNAi-based chemical genetic screen identifies three small-molecule inhibitors of the Wnt/wingless signaling pathway. *Proc. Natl. Acad. Sci. U.S.A.* **2011**, *108*, 5954–5963.

(18) Trosset, J.-Y.; Dalvit, C.; Knapp, S.; Fasolini, M.; Veronesi, M.; Mantegani, S.; Gianellini, L. M.; Catana, C.; Sundström, M.; Stouten, P. F. W.; Moll, J. K. Inhibition of protein-protein interactions: The discovery of druglike  $\beta$ -catenin inhibitors by combining virtual and biophysical screening. *Proteins* **2006**, *64*, 60–67.

(19) Tian, W.; Han, X.; Yan, M.; Xu, Y.; Duggineni, S.; Lin, N.; Luo, G.; Li, Y. M.; Han, X.; Huang, Z.; An, J. Structure-based discovery of a novel inhibitor targeting the  $\beta$ -catenin/Tcf4 interaction. *Biochemistry* **2012**, *51*, 724–731.

(20) Yu, B.; Huang, Z.; Zhang, M.; Dillard, D. R.; Ji, H. Rational design of small-molecule inhibitors for  $\beta$ -catenin/T-cell factor protein-protein interactions by bioisostere replacement. *ACS Chem. Biol.* **2013**, DOI: 10.1021/cb300564v.

(21) Choi, H.-J.; Gross, J. C.; Pokutta, S.; Weis, W. I. Interactions of plakoglobin and  $\beta$ -catenin with desmosomal cadherins: basis of selective exclusion of  $\alpha$ - and  $\beta$ -catenin from desmosomes. *J. Biol. Chem.* **2009**, *284*, 31776–31788.

(22) Zhang, M.; Huang, Z.; Yu, B.; Ji, H. New homogeneous high-throughput assays for inhibitors of  $\beta$ -catenin/Tcf protein-protein interactions. *Anal. Biochem.* **2012**, *424*, 57–63.